2017 IEEE International Conference on Systems, Man, and Cybernetics (SMC)
Banff Center, Banff, Canada, October 5-8, 2017

Inverse solutions for Brain-Computer Interfaces: Effects of regularisation on localisation and classification

Mohit Kumar Goel, Ricardo Chavarriaga† and José del R. Millán
Chair on Non-Invasive Brain-Machine Interface (CNBI), Center for Neuroprosthetics, School of Engineering,
Ecole Polytechnique Fédérale de Lausanne, Switzerland
†ricardo.chavarriaga@epfl.ch

***Abstract*—Estimation of intracranial sources, using inverse solutions methods, has been proposed as a mean to improve performance in non-invasive brain-computer interfaces. These methods estimate the activity of a large number of neural sources from a smaller number of scalp electroencephalography (EEG) channels. This is a highly undetermined problem and regularisation constraints need to be applied. In this paper we compared the effect of several regularisation constraints and parameters in the localisation error and classification performance. Results on three event-related potential protocols –rapid serial visual processing, P300-speller and error-related potentials– showed no significant difference in the maximum performance between minimum norm or weighted minimum norm regularisation constraints. Standardised methods despite yielding lower localisation error resulted in decreased classification performance. Noteworthy, testing on data acquired in different days than the training suggests that discriminant features extracted from intracranial sources are stable across sessions.**

I. Introduction

Brain computer interfaces (BCIs) aim at providing an alternate means of communication and control by direct decoding of brain activity [1], [2]. The electroencephalogram (EEG) is the most common recording technique due to its non-invasiveness, affordability and portability [3], [4]. EEG signals, however, suffer from low spatial resolution due to poor skull conductivity which smears the electrical activity when conducted from the cortical sources to the scalp [5], [6]. This results in low signal-to-noise (SNR) ratio of EEG recordings which poses a serious challenge for BCI systems to accurately recognise different mental states.

The estimation of intracranial activity, by computing the inverse solution [7]–[9] has been proposed as a mean to obtain better classification performance compared to surface EEG [10]–[12], [12]–[14]. The rationale is to increase spatial resolution of EEG by projecting scalp potentials onto a higher dimensional space corresponding to a large number of cortical sources [5]. The estimated activity for these sources is expected to have better signal to noise ratio as they represent unmixed scalp potentials captured by the EEG electrodes. From a classification perspective, the assumption is that features extracted from the estimated source activity will have better discrimination between the different BCI classes.

In this paper we assessed different inverse solution methods on three Event-Related Potential (ERP) based BCI experiments (c.f., Figure 1): Rapid Serial Visual Presentation (RSVP) [15], P300-speller [16] and Error-related Potential (ErrP) [17]. More specifically, we used offline analysis to compare different regularisation constraints and parameters of the inverse solution in terms of the localisation error and the decoding performance

II. Methods

A. Experimental protocols

In the RSVP protocol subjects (N=10) are asked to observe a sequence of images (presentation rate: 4 images per second) and be attentive to the appearance of images of a given target class [15]. The evoked EEG activity is decoded to differentiate between target and distractor images. Training data was acquired during 4 search tasks, each one composed of two sequences of 200 images. The testing phase, recorded on the same day, comprised three search tasks using different target objects than in training. We recorded 64 EEG channels (f_s:2048 Hz; filtered [1-10 Hz]; CAR re-referenced; and downsampled to 32Hz). For classification we used the activity in the time window [200-700] ms post stimulus.

The P300-speller experiment (N=8) was performed over two days (average separation of 12 days); each day an average of 5 runs (each run comprised writing of 5 characters) were performed per subject. Data of the first day was used as training dataset and the second day was used for testing. Recordings included 61 EEG channels (f_s:250Hz; filtered [1 20] Hz; CAR referenced; and downsampled to 50 Hz). Signal in the window [100 600] ms was selected for classification.

In the ErrP experiment subjects (N=6) observed a cursor that moves horizontally towards a target location [17]. 20% of the time the cursor moved in the direction away from the target. The experiment was performed over two days and data from the first day was used as training set; while the second day was used for testing. Recordings included 64 EEG channels (f_s:2048 Hz; filtered [1-10] Hz; CAR referenced; and downsampled to 32Hz). Classification was based on the data in the time window [200-450] ms.

B. Estimation of intracranial sources and regularisation

In general terms, the activity of intracranial sources ($\mathbf{x}$), i.e. the inverse solution problem, is estimated using a linear

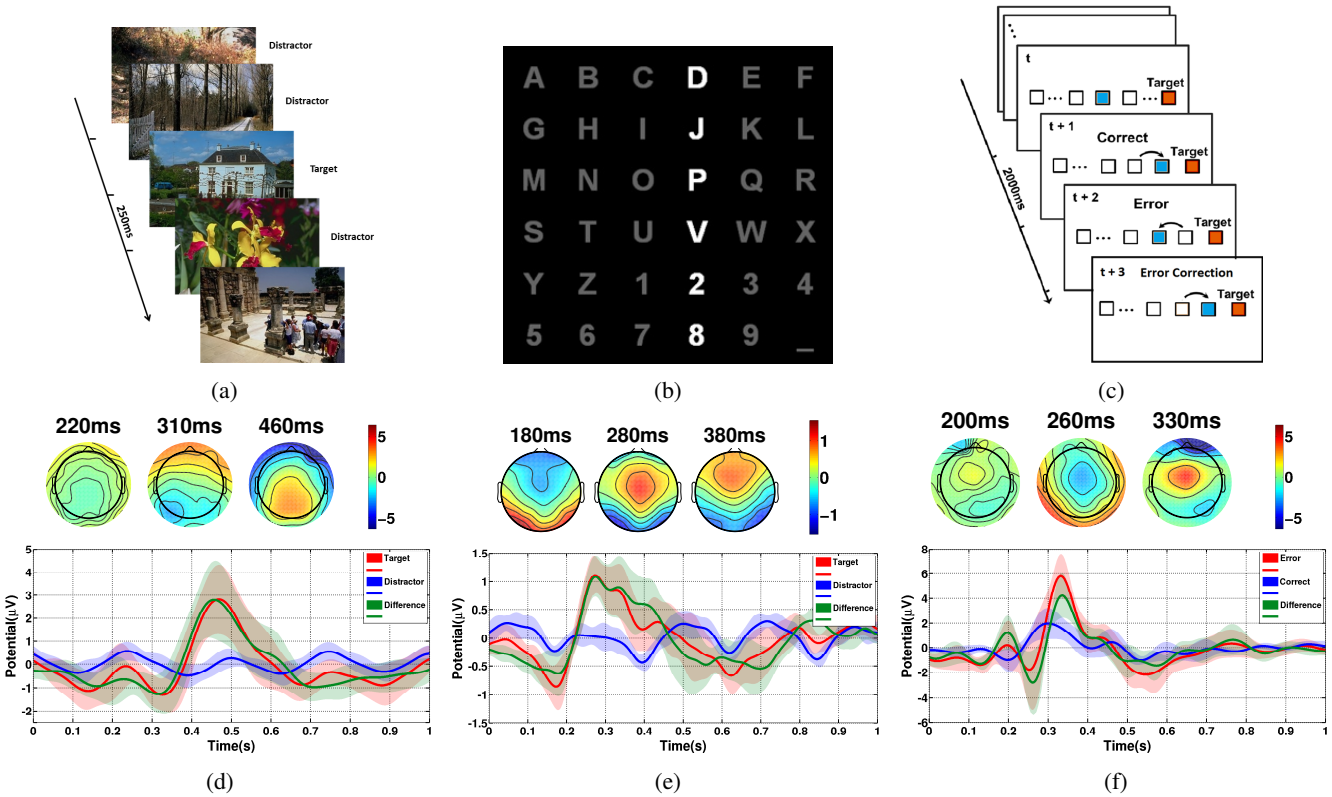

Fig. 1: *Top*. Experimental protocols. (a) RSVP experiment where a sequence of images is presented at 4 Hz. Here the target is 'car' and the remaining images correspond to distractors. (b) P300-speller where 6x6 matrix of letters and numbers are used. Note that 4^{th} column is highlighted in this image. (c) ErrP Experiment. The curly arrow shows the movement of the blue cursor committing error and being rectified in the next step for online implementation. *Bottom* Grand average ERP, mean and standard variation for both conditions and their difference. Topographic representation of scalp-wide activity is shown at selected time points. (d) RSVP experiment. Pz electrode; N=10. (e) P300-speller. Cz electrode; N=8. (f) ErrP experiment. FCz electrode; N=6.

transformation of surface EEG potential ($\mathbf{b}$) at a given time t as,

$$\mathbf{x}(t) = \mathbf{G}\mathbf{b}(t) \tag{1}$$

where $\mathbf{G}$ is a matrix that represents the inverse of a forward model,

$$\mathbf{b}(t) = \mathbf{A}\mathbf{x}(t) \tag{2}$$

which emulates the electrical propagation properties from the cortical sources to surface EEG potentials. For more details on inverse solutions please refer to [7], [13], [18].

The term $\mathbf{G}$ in Equation 1 corresponds to the pseudo-inverse matrix obtained by minimisation of the following cost function [19]

$$\xi = \arg\min_{x} \left(\|\mathbf{A}\mathbf{x} - \mathbf{b}\|_M^2 + \lambda \|\mathbf{x}\|_N^2 \right) \tag{3}$$

The first term $\|\mathbf{A}\mathbf{x} - \mathbf{b}\|$ (data space) represents the energy of error in estimating the scalp EEG from the intracranial sources. The second term $\|\mathbf{x}\|$ (source space) represents the energy of the sources. It is added as a *regularisation* term to constraint the range of $\mathbf{x}$ in the final solution (see below). The parameters $\mathbf{M}$ and $\mathbf{N}$ represent the metric for the data space and the source space, respectively, while λ balances the two energy terms.

The inverse problem is highly underdetermined since it estimates the current density of a large number of dipolar sources from a few surface channels. For this reason, regularisation constraints–often based on bio-physical properties of the brain–are introduced in the inverse equation to restrict the range of allowable solutions. In consequence, various distributed inverse solutions have been proposed in the literature. They differ on the basis of regularisation constraints and the choice of the forward head model. The *Minimum Norm Estimation* (MNE) solution [20] assumes that current distribution in the dipolar sources should have limited overall intensity while simultaneously fitting the data. It defines $\mathbf{N}$ as the identity matrix. This algorithm penalises estimation of strong activity of the solution points and privileges weak, localised activation patterns. Consequently, the superficial sources are favoured by MNE algorithm, while deeper sources can be incorrectly projected near the surface. To compensate for this effect, different *Weighted Minimum Norm* based solutions have been proposed. The most common of them allocates

higher weights obtained from the column norm of leadfield matrix, $(\mathbf{N}^{-1})_{ii} = \|\mathbf{A}_i\|^{-2}$ [21]. The acronym WMN has become synonymous with this approach. Well-known methods using this approach include Cortical current Density (CCD), which combines WMN and a forward model composed of dipoles arranged on the cortical surface [13]; and LORETA [22] which implements a Laplacian WMN that ensures maximum smoothness of the solution, based on the assumption that neighbouring areas are simultaneously and synchronously activated. Furthermore, it has been shown that standardisation over MNE (sLORETA) reduces the source localisation error in the case of low noise [23].

In this work we assessed the effect on both the localisation error and the decoding of the ERP patterns of four different regularisation constraints, as follows:

1) *MNE* ($\mathbf{N} = \mathbf{I}$)

$$\mathbf{G} = \mathbf{A}'(\mathbf{A}\mathbf{A}' + \lambda\mathbf{M}^{-1})^{-1} \tag{4}$$

2) *Depth-WMN* ($\mathbf{N}_{ii} = ||\mathbf{A}_i||^2$)

$$\mathbf{G} = \mathbf{N}^{-1}\mathbf{A}'(\mathbf{A}\mathbf{N}^{-1}\mathbf{A}' + \lambda\mathbf{I})^{-1} \tag{5}$$

3) *Standardised MNE (sMNE)*

$$\mathbf{G} = (\mathbf{A}'(\mathbf{A}\mathbf{A}' + \lambda\mathbf{I})^{-1}\mathbf{A})^{-1/2}.\mathbf{A}'(\mathbf{A}\mathbf{A}' + \lambda\mathbf{I})^{-1} \tag{6}$$

4) *Standardised depth-WMN (sWMN)*

$$\begin{aligned}\mathbf{G} = (\mathbf{N}^{-1}\mathbf{A}'(\mathbf{A}\mathbf{N}^{-1}\mathbf{A}' + \lambda\mathbf{I})^{-1}\mathbf{A})^{-1/2} \\ .\mathbf{N}^{-1}\mathbf{A}'(\mathbf{A}\mathbf{N}^{-1}\mathbf{A}' + \lambda\mathbf{I})^{-1}\end{aligned} \tag{7}$$

For this comparison we used a head model assuming cortical activity in form of dipoles which are perpendicularly arranged on the cortical surface with fixed orientation [24]. The geometry of the cortical mantle –obtained from the average brain of the Montreal Neurological Institute [25]– is divided into 3013 vertices, each representing a dipolar source. We systematically assessed the regularisation effect by changing the λ parameter in the range $[10^{-7}\ 10^{7}]$.

C. Localisation error

We evaluated how the parameter λ affects the localisation error for the four regularisation constraints mentioned in the previous section. It follows the procedure described by Michel et al. [8], in which the forward model is used to obtain an intermediary surface EEG data by activating one dipole at a time among all the dipoles in the model. Next, white noise is added corresponding to noise ranging from 0 dB to 1000 dB to obtain the resultant surface EEG data. The value 1000 dB effectively represents a noiseless scenario. Similar range has been considered in [26]. Subsequently, the inverse method is used to localise the artificial surface EEG data by choosing the dipole with highest estimated strength. Finally, the localisation error E is computed as follows

$$E = \frac{1}{N}\sum_{n=1}^{N}|r_{loc_n} - r_{sim_n}| \tag{8}$$

where, r_{loc} and r_{sim} are the coordinates of localised and simulated dipoles, respectively. N is the total number of simulated dipoles.

D. Feature selection and classification

Estimation of intracranial sources yields a high-dimensional representation of the ERP response (corresponding to the activity of the 3013 sources at each time point). In order to identify the most discriminant cortical sources we computed the Fisher score [27], [28]

$$S_i = \frac{\mu_{i1} - \mu_{i2}}{\sigma_{i1}^2 + \sigma_{i2}^2} \tag{9}$$

where, μ_{ij} and σ_{ij}^2 are mean and covariance respectively, for data distribution from source i (up to 3013 sources) and class $j(= 1, 2)$. In equation 9, the score S is higher for those sources whose data distribution for the two classes have a large separation between their means and have small intra-class variance.

Taking into account that each selected feature in the inverse space is already a linear combination of potentials from all surface EEG electrodes, we used an ensemble approach where classifiers built for each feature are fused together. This approach relies on the combination of weak classifiers to obtain a more reliable decoding [29]. Moreover, using one classifier per feature reduces the possibility of overfitting with limited number of trials compared to using a single classifier that combines many features.

The classification result for a feature $x_i\ (i = 1, 2, ..., D)$ is obtained as the probability of likelihood to the training means and covariance,

$$P(\omega_j|x_i(t)) = \frac{1}{\sqrt{2\pi\sigma_{ij}^2(t)}}e^{-\frac{(x_i(t)-\mu_{ij}(t))^2}{2\sigma_{ij}^2(t)}} \tag{10}$$

where $\mu_{ij}(t)$ and $\sigma_{ij}(t)$ are mean and covariance for the data of class $\omega_j\ (j = 1, 2)$. The probability $P(\omega_j|\mathbf{x}(t))$ at time t is computed by combining the output for all the sources,

$$P(\omega_j|\mathbf{x}(t)) \quad = \quad \prod_{i=1}^{D} P(\omega_j|x_i(t)) \tag{11}$$

where D is the number of selected discriminant sources at time t. In this study we use $D = 100$ for all cases. The final decision for a trial is made by combining all the probabilities using again Naïve Bayes rule [27] for two classes over the selected time window of data.

$$P(\omega_j|\mathbf{x}) \quad = \quad \prod_{t=1}^{T} P(\omega_j|\mathbf{x}(t)) \tag{12}$$

We assessed the effect of the regularisation constraint and parameter λ on the classification performance for BCI. We report performance in terms of the the area under the specificity-sensitivity curve (AUC) [30] computed using 4-fold cross-validation in data from the training session, as well as the performance on the testing session, in order to assess the generalisation of the decoding process.

III. Results

The three experimental protocols yielded ERP consistent with the literature as shown in Figure 1.

A. Localisation error

Figure 2 shows the average localisation error for different values of regularisation parameter λ and SNR. In the case of MNE and sMNE, for λ in the range $[10^{-2}\ 10^{2}]$ we see a decrease in the localisation error. In the case of low noise levels the error yielded minimum values between 10^{0} and 10^{2} in the case of MNE. For sMNE the error remains at minimum value for $\lambda > 10^{2}$. Similarly, WMN and sWMN exhibited changes in the localisation error when λ varies in the range $[10^{-1}\ 10^{3}]$. The localisation error is largely unaffected for values outside this range. This coincides with previous analysis of WMN [31].

Overall, the minimum localisation error was achieved with sMNE ($= 0, \lambda \in [10^{-7}\ 10^{7}], SNR \geq 100$) while the other methods, MNE, WMN and sWMN, yielded a minimal error of about 30 mm on average ($\lambda \in [10^{-7}\ 10^{2}], SNR \geq 100$). The standard deviation at each point in the graph is around 30mm (not shown for sake of clarity), consistent with similar studies [7]. The maximum localisation errors in all methods in the case of low SNR is equivalent to random localisation.

The effect of standardization in localisation error is clearly evident for sMNE but not for sWMN approach. sMNE, which is popularly known as sLORETA [23], achieves zero localisation error over the whole range of λ for SNR above 100dB. In comparison, standardization over WMN does not reduce localisation error to zero, although it does reduce the level of localisation error for $\lambda < 10^{-4}$ when SNR is around 50 dB.

B. Classification

The top row of Fig. 3 show the result of cross-validation analysis for the three experiments. The top row shows the AUC yielded by cross-validation in the training session. Performance reaches a peak value in the same range of λ values; i.e. $[10^{-2}\ 10^{2}]$ for MNE and sMNE and $[10^{-1}\ 10^{3}]$ for WMN and sWMN methods. The range of λ values for maximum AUC seems to be invariant of the experimental protocol and highly consistent across the subjects. For each case, The peak AUC was significantly higher than for other λ values in the three protocols ($p < 0.001$; 1-way ANOVA repeated measure). Performance of the standardised constraints (sMNE and SWMN) were consistently lower in all cases. No significant differences ($p > 0.05; t\text{–}test$) were found when comparing average classification performance using MNE or WMN. Similarly no difference was found between sMNE and sWMN methods.

We then evaluated the stability of the classification process by assessing performance in the testing session. Results are shown in the bottom row of Fig. 3. Peak AUC values in the testing session are observed in the same range of λ values as in the cross-validation analysis. However, performance seems less sensitive to the value of λ. As before, the standardisation decreases the classification performance. In the cases of the ErrP and P300, performance is close to chance level, in particular for $\lambda < 1$. No significant difference was found between the peak AUC for MNE and WMN methods for

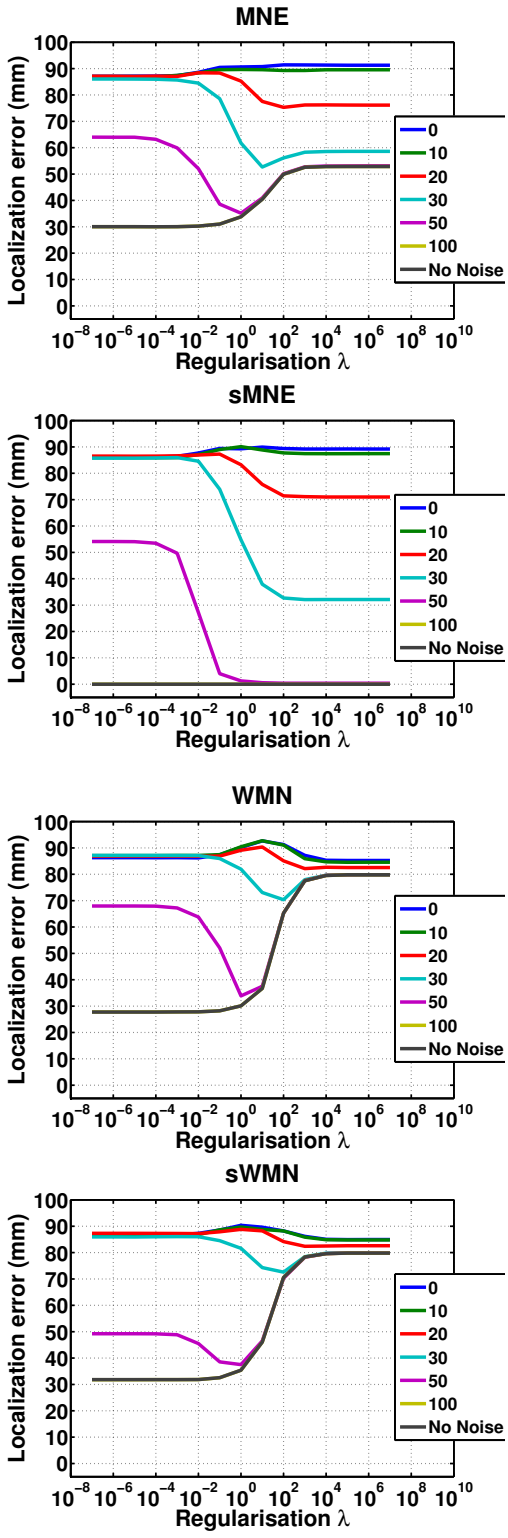

Fig. 2: Localisation error for different values of the regularisation parameter and inverse methods. Each trace corresponds to a different SNR (in dB). The trace for 'No Noise' overlaps SNR=100dB, showing no change in localisation for SNR $>$ 100dB.

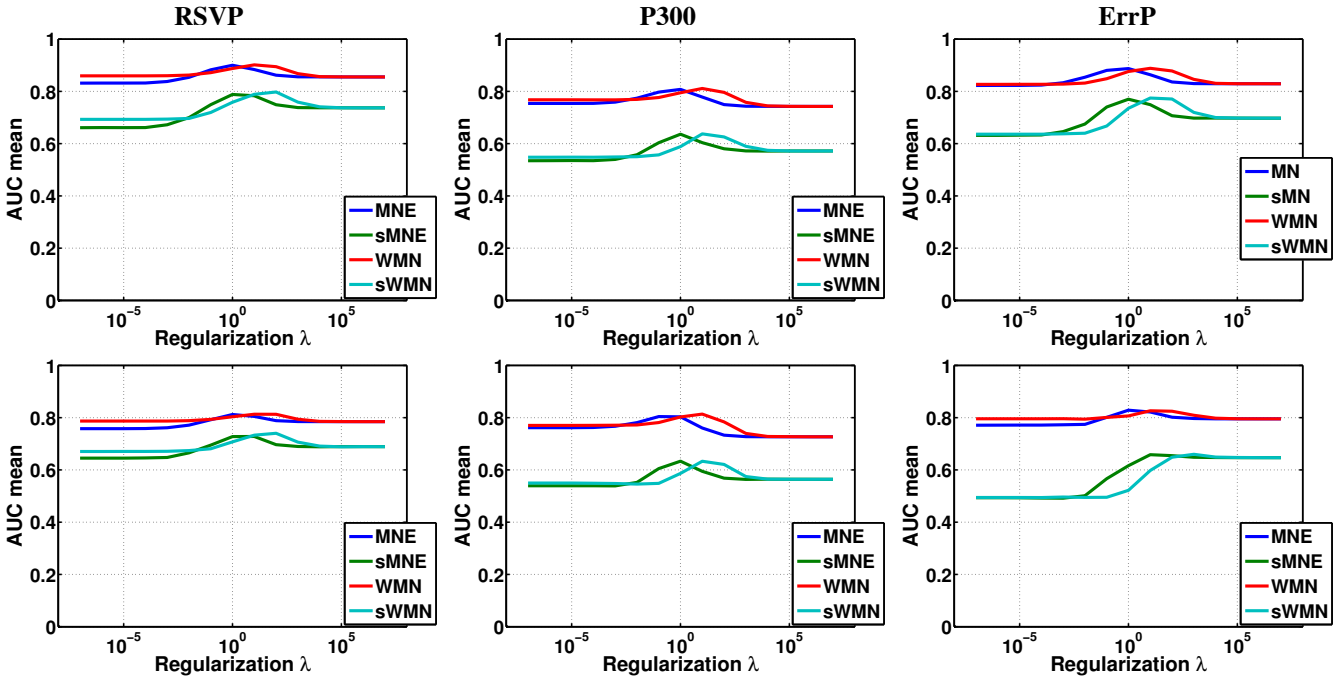

Fig. 3: Performance in the three protocols. *Top*: AUC Cross-validation. *Bottom*: AUC - Testing dataset. Mean across all subjects.

the three experiments ($p > 0.05; t\text{–}test$), as well as between sMNE and sWMN methods ($p > 0.05; t\text{–}test$).

IV. Conclusion

The use of inverse solutions in BCI is affected by the choice of two free parameters, namely, the type of regularisation constraint and the regularisation parameter λ. Our results show that the value for regularisation parameter λ that yields maximum classification performance is constant across subjects and largely independent of the experimental protocol. No difference was found for the maximum performance obtained using MNE or WMN. In contrast, results for the three experiments show that the standardised methods (sMNE and sWMN) consistently yield significantly lower classification performance compared to their non-standardised counterparts. The standardisation changes the variance of the whole data which results in increased overlapping of distribution for the individual classes and subsequent reduction in classification performance.

It is worth noticing that the within-session and across-session performance in MNE and WMN was similar. This suggest that discriminant activity in features extracted from the intracranial sources are rather stable. Importantly, in the P300 and ErrP protocols the training and testing sessions were performed in different days which further supports the possibility of using these features for ERP-based BCI applications. Further analysis is required to evaluate if similar conclusions are achieved in the case of asynchronous BCI systems (e.g. those based on self-paced sensory-motor rhythms).

Regarding localisation of intracranial sources, the lowest localisation error is obtained with the standardised MNE, which in turn, yields lower classification performance. In contrast, MNE achieves high classification performance at the cost of poor localisation accuracy, in particular for deeper sources. In this regard, depth-WMN based method provides a good trade-off choice for performing both classification and localisation analysis since its classification performance is comparable to MNE while it has constraints to localise deeper sources. Nevertheless, in the present study WMN –giving more weight to deeper sources– did not result in smaller localisation error compared to MNE. This can be due to the use of a forward model with dipolar sources arranged on the cortical surface.

Acknowledgment

This study is supported by the SNSF grant 200021-120293, and the SNSF-funded NCCR-robotics. We thank Fabio Aloise and the IRCCS Fondazione Santa Lucia, Rome for providing the P300 dataset.

References

[1] J. d. R. Millán, R. Rupp, G. Müller-Putz, R. Murray-Smith, C. Giugliemma, M. Tangermann, C. Vidaurre, F. Cincotti, A. Kübler, R. Leeb, C. Neuper, K. Müller, and D. Mattia, "Combining brain-computer interfaces and assistive technologies: State-of-the-art and challenges," *Frontiers in Neuroscience*, vol. 4, p. 161, 2010.

[2] J. R. Wolpaw, N. Birbaumer, D. J. McFarland, G. Pfurtscheller, and T. M. Vaughan, "Brain-computer interfaces for communication and control," *Clinical Neurophysiology*, vol. 113, no. 6, pp. 767–791, Jun 2002.

[3] J. R. Wolpaw, "Brain-computer interfaces as new brain output pathways," *Journal of Physiology*, vol. 579, no. Pt 3, pp. 613–619, Mar 2007. [Online]. Available: http://dx.doi.org/10.1113/jphysiol.2006.125948

[4] J. d. R. Millán and J. Carmena, "Invasive or Noninvasive: Understanding Brain-Machine InterfaceTechnology," *IEEE engineering in Medicine and Biology magazine*, vol. 29, pp. 16–22, 2010.

[5] R. Srinivasan, "Methods to improve the spatial resolution of EEG," *International Journal of Bioelectromagnetism*, vol. 1, pp. 102–111, 1999.

[6] P. L. Nunez, *Electric Fields of the Brain: The Neurophysics of EEG*. New York: Oxford University Press, 1981.

[7] R. Grech, T. Cassar, J. Muscat, K. P. Camilleri, S. G. Fabri, M. Zervakis, P. Xanthopoulos, V. Sakkalis, and B. Vanrumste, "Review on solving the inverse problem in EEG source analysis," *Journal of NeuroEngineering and Rehabilitation*, vol. 5, p. 25, 2008.

[8] C. M. Michel, M. M. Murray, G. Lantz, S. Gonzalez, L. Spinelli, and R. Grave de Peralta Menendez, "EEG source imaging," *Clinical Neurophysiology*, vol. 115, pp. 2195–2222, 2004.

[9] S. Baillet, J. C. Mosher, and R. M. Leahy, "Electromagnetic brain mapping," *IEEE Signal Processing Magazine*, vol. 18, pp. 14–30, 2001.

[10] R. Grave de Peralta Menendez, S. L. Gonzalez Andino, L. Perez, P. W. Ferrez, and J. d. R. Millán, "Non-invasive estimation of local field potentials for neuroprosthesis control," *Cognitive Processing*, vol. 6, pp. 59–64, 2005. [Online]. Available: http://www.springerlink.com/content/dqwpmgh4wj7kjdx9/

[11] Q. Noirhomme, R. I. Kitney, and B. Macq, "Single-trial EEG source reconstruction for brain-computer interface," *IEEE Transactions on Biomedical Engineering*, vol. 55, pp. 1592–1601, 2008.

[12] F. Lotte, A. Lécuyer, and B. Arnaldi, "FuRIA: An inverse solution based feature extraction algorithm using fuzzy set theory for brain-computer interfaces," *IEEE Transactions on Signal Processing*, vol. 57, no. 8, pp. 3253–3263, 2009.

[13] F. Cincotti, D. Mattia, F. Aloise, S. Bufalari, L. Astolfi, F. D. V. Fallani, A. Tocci, L. Bianchi, M. G. Marciani, S. Gao, J. d. R. Millán, and F. Babiloni, "High-resolution EEG techniques for brain-computer interface applications," *Journal of Neuroscience Methods*, vol. 167, no. 1, pp. 31–42, Jan 2008. [Online]. Available: http://dx.doi.org/10.1016/j.jneumeth.2007.06.031

[14] G. Garipelli, R. Chavarriaga, F. Cincotti, F. Babiloni, and J. d. R. Millán, "Discriminative channel selection method for the recognition of anticipation related potentials from CCD estimated cortical activity," in *Proceeding of IEEE International Worshop on MLSP*, 2009. [Online]. Available: http://mlsp2009.conwiz.dk/

[15] M. Uscumlic, R. Chavarriaga, and J. Milln, "An iterative framework for EEG-based image search: Robust retrieval with weak classifiers," *PLoS ONE*, vol. 8, p. e72018, 2013.

[16] L. A. Farwell and E. Donchin, "Talking off the top of your head: toward a mental prosthesis utilizing event-related brain potentials," *Electroencephalography and Clinical Neurophysiology*, vol. 70, pp. 510–523, 1988.

[17] R. Chavarriaga and J. d. R. Millán, "Learning from EEG Error-related Potentials in Noninvasive Brain-Computer Interfaces." *IEEE Transactions on Neural System Rehabilitation Engineering*, vol. 18, pp. 381–388, 2010.

[18] F. Babiloni, C. Babiloni, L. Locche, F. Cincotti, P. M. Rossini, and F. Carducci, "High-resolution electro-encephalogram: Source estimates of Laplacian-transformed somatosensory-evoked potentials using a realistic subject head model constructed from magnetic resonance images," *Medical & Biological Engineering & Computing*, vol. 38, pp. 512–519, 2000.

[19] R. A. Willoughby, "Solutions of ill-posed problems (A. N. Tikhonov and V. Y. Arsenin)," *SIAM Review*, vol. 21, no. 2, pp. 266–267, 1979. [Online]. Available: http://link.aip.org/link/?SIR/21/266/1

[20] M. S. Hmlinen and R. J. Ilmoniemi, "Interpreting magnetic fields of the brain: minimum norm estimates." *Medical & Biological Engineering & Computing*, vol. 32, no. 1, pp. 35–42, Jan 1994.

[21] C. L. Lawson and R. J. Hanson, *Solving least squares problems*. Englewood Cliffs: Prentice-Hall, 1974.

[22] R. D. Pascual-Marqui, C. Michel, and D. Lehmann, "Low-resolution electromagnetic tomography: A new method for localizing electrical activity in the brain," *International Journal of Psychophysiology*, vol. 18, pp. 49–65, 1994.

[23] R. D. Pascual-Marqui, "Standardized low-resolution brain electromagnetic tomography (sLORETA): Technical details," *Methods & Findings in Experimental & Clinical Pharmacology*, vol. 24D, pp. 5–12, 2002.

[24] A. M. Dale and M. I. Sereno, "Improved localization of cortical activity by combining EEGand MEG with MRI cortical surface reconstruction: A linear approach," *Journal of Cognitive Neuroscience*, vol. 5, no. 2, pp. 162–176, Apr. 1993. [Online]. Available: http://dx.doi.org/10.1162/jocn.1993.5.2.162

[25] M. Fuchs, J. Kastner, M. Wagner, S. Hawes, and J. S. Ebersole, "A standardized boundary element method volume conductor model," *Clinical Neurophysiology*, vol. 113, no. 5, pp. 702–712, 2002. [Online]. Available: http://www.sciencedirect.com/science/article/B6VNP-45B685N-4/2/9e72171e12c80f7d9b3106c6ddcd5b93

[26] F. Babiloni, C. Babiloni, F. Carducci, G. L. Romani, P. M. Rossini, L. M. Angelone, and F. Cincotti, "Multimodal integration of high-resolution EEG and functional magnetic resonance imaging data: a simulation study," *NeuroImage*, vol. 19, no. 1, pp. 1–15, 2003. [Online]. Available: http://www.sciencedirect.com/science/article/B6WNP-487DJMP-3/2/0e61efd567f27520725916a5b688371a

[27] R. O. Duda, P. E. Hart, and D. G. Stork, *Pattern Classification (2nd Edition)*, 2nd ed. Wiley-Interscience, November 2000. [Online]. Available: http://www.worldcat.org/isbn/0471056693

[28] C. S. Dhir and S. Y. Lee, *Advances in Neuro-Information Processing*, M. Kppen, N. Kasabov, and G. Coghill, Eds. Springer Berlin Heidelberg, 2009.

[29] R. Polikar, "Ensemble based systems in decision making," *IEEE Circuits and Systems Magazine*, vol. 6, no. 3, pp. 21–45, 2006.

[30] T. Fawcett, "An introduction to ROC analysis," *Pattern Recognition Letters*, vol. 27, no. 8, pp. 861 – 874, 2006, rOC Analysis in Pattern Recognition.

[31] C. Phillips, M. D. Rugg, and K. J. Friston, "Systematic regularization of linear inverse solutions of the EEG source localization problem," *NeuroImage*, vol. 17, no. 1, pp. 287–301, 2002. [Online]. Available: http://www.sciencedirect.com/science/article/B6WNP-47DKV9V-R/2/67a6a338f7afc420dc6ea78c22b5eff4